

## Electronic-structure-induced reconstruction and magnetic ordering at the $\text{LaAlO}_3/\text{SrTiO}_3$ interface

This content has been downloaded from IOPscience. Please scroll down to see the full text.

2008 EPL 84 27001

(<http://iopscience.iop.org/0295-5075/84/2/27001>)

View [the table of contents for this issue](#), or go to the [journal homepage](#) for more

Download details:

IP Address: 61.129.42.14

This content was downloaded on 11/05/2016 at 08:45

Please note that [terms and conditions apply](#).

# Electronic-structure-induced reconstruction and magnetic ordering at the $\text{LaAlO}_3|\text{SrTiO}_3$ interface

ZHICHENG ZHONG<sup>(a)</sup> and PAUL J. KELLY<sup>(b)</sup>

*Faculty of Science and Technology and MESA<sup>+</sup> Institute for Nanotechnology, University of Twente  
P.O. Box 217, 7500 AE Enschede, The Netherlands*

received on 27 August 2008; accepted by E. Bertel on 1 September 2008

published online 10 September 2008

PACS 75.70.Cn – Magnetic properties of interfaces (multilayers, superlattices, heterostructures)

PACS 73.20.-r – Electron states at surfaces and interfaces

PACS 68.35.Ct – Interface structure and roughness

**Abstract** – Using local density approximation (LDA) calculations we predict **GdFeO<sub>3</sub>-like rotation of TiO<sub>6</sub> octahedra at the *n*-type interface between LaAlO<sub>3</sub> and SrTiO<sub>3</sub>. This results in a narrowing of the Ti *d* bandwidth by 1/3 so that LDA + *U* calculations predict an antiferromagnetic, charge- and spin-ordered ground state for very modest values of *U*.** Recent experimental evidence for magnetic interface ordering may be understood in terms of **the close proximity of an antiferromagnetic insulating ground state to a ferromagnetic metallic excited state.**

Copyright © EPLA, 2008

Transition metal (TM) oxides in bulk form exhibit a huge range of physical properties. Heterostructures of TM oxides offer the prospect of greatly enhancing these properties or of combining them to realize entirely new properties and functionalities. The recent finding that a  $\text{TiO}_2|\text{LaO}$  interface between the insulating oxides  $\text{LaAlO}_3$  and  $\text{SrTiO}_3$  can be metallic with an extremely high carrier mobility [1] has triggered a surge of experimental and theoretical studies of this interface [2–12]. The valence mismatch at the interface leads to the transfer of half an electron per unit cell from  $\text{LaAlO}_3$  (LAO: band gap 5.6 eV) to  $\text{SrTiO}_3$  (STO: band gap 3.2 eV), from the LaO interface layer to the  $\text{TiO}_2$  layer. For a defect-free interface, the concentration of these “intrinsic” sheet carriers is  $n_{\text{sheet}} \approx 3.3 \times 10^{14} \text{ cm}^{-2}$ . For samples prepared under low oxygen pressure ( $< 10^{-4}$  mbar), the carrier density is much larger than this intrinsic value, suggesting that their properties are determined by extrinsic carriers related to oxygen vacancies formed in the STO substrate during the growth of the LAO film.

Samples prepared under increasing oxygen pressure exhibit a large increase of the sheet resistance [1,4,6,13]. A sheet resistance which decreases on increasing the temperature from 10 K to 70 K, large negative magnetoresistance and magnetic hysteresis at low temperatures were found in ref. [4] and these properties are presumably

characteristic of intrinsic interfaces. The partial filling of the Ti *d* states at the *n*-type interface means that locally the electronic structure is intermediate between orthorhombic  $\text{LaTiO}_3$  ( $\text{Ti}^{3+}$ ) and cubic  $\text{SrTiO}_3$  ( $\text{Ti}^{4+}$ ).  **$\text{LaTiO}_3$  (LTO) is a G-type antiferromagnetic (AFM) Mott insulator with a Néel temperature of 146 K [14–16] and a band gap of 0.2 eV [17].** Compared to cubic STO, the additional electron in the  $t_{2g}$  conduction band state on the Ti ion leads to **a GdFeO<sub>3</sub>-type crystal structure (space group *Pbnm*) which can be derived from the ideal perovskite cubic structure by tilting essentially ideal  $\text{TiO}_6$  octahedra about the *b*-axis followed by a rotation about the *c*-axis (see fig. 1).**

**In this paper we suggest that GdFeO<sub>3</sub>-type distortions at LAO|STO interfaces play an essential role in reducing the bandwidth of the occupied interface Ti *d* state by one-third, making it more sensitive to on-site Coulomb correlations and stabilizing an antiferromagnetic ground state.** Surprisingly little attention has been paid to the possibility of such distortions at the LAO|STO interface. Theoretical studies have been largely concerned with explaining the metallic behavior of *n*-type and the insulating character of *p*-type interfaces [11,12,18–20] with most emphasis being placed on the charge transfer between the LaO and  $\text{TiO}_2$  interface layers.

Though LDA total energy calculations describe equilibrium crystal structures with good accuracy and have been applied extensively to non-metallic TM oxides [21], we are not aware of them being used to predict the

<sup>(a)</sup>E-mail: z.c.zhong@utwente.nl

<sup>(b)</sup>E-mail: P.J.Kelly@tnw.utwente.nl

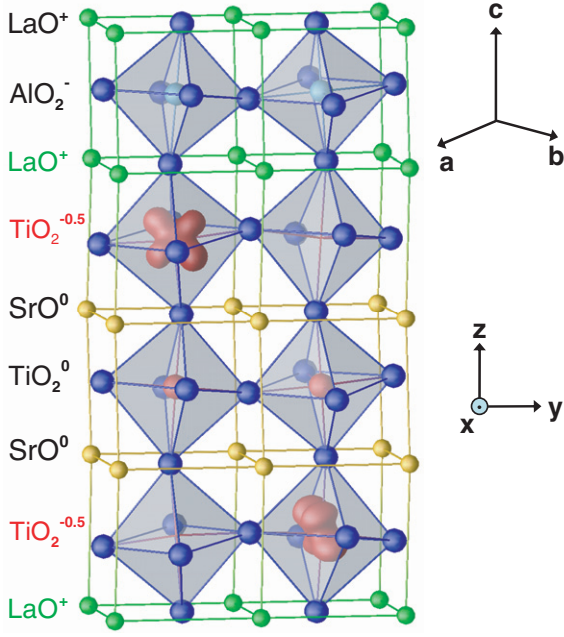


**Fig. 1:** (Colour on-line) Relaxed  $\text{LaAlO}_3|\text{SrTiO}_3$  interface structure and charge density iso-surface of the surplus electron for the **charge-ordered ferromagnetic state**. The orthorhombic translation vectors are **a, b, c**.

structures of open-shell correlated solids. To establish a predictive capability for the LAO|STO system, we carried out a systematic study of the crystal structure of the  $3d^1$  perovskites  $\text{CaVO}_3$ ,  $\text{SrVO}_3$ ,  $\text{YTiO}_3$  and  $\text{LaTiO}_3$ . We could show that LDA calculations reproduce the well-documented [22]  $\text{GdFeO}_3$ -type distortions in this system very well. To study various types of magnetic ordering, we took account of the Coulomb interaction of the partially filled  $d$ -shell using a local Coulomb interaction parameter  $U_d$  [23] which has been shown to describe the ground state of  $\text{YTiO}_3$  and  $\text{LaTiO}_3$  qualitatively correctly [24]. The LDA +  $U$  results are in even closer agreement with experiment [25].

**Method.** – We model the LAO|STO interface using a periodically repeated  $(m, n)$  supercell containing  $m$  layers of LAO and  $n$  layers of TiO. Most of the results to be reported below were obtained with the 40-atom  $c(2 \times 2)$  ( $\frac{3}{2}, \frac{5}{2}$ ) supercell depicted in fig. 1 containing two  $n$ -type interfaces, and did not change significantly when a  $(\frac{5}{2}, \frac{7}{2})$  supercell was used instead. To study AFM ordering the above supercell was doubled in the  $xy$ -plane leading to a  $p(2 \times 2)$  unit cell containing 80 atoms.

The LDA and LDA +  $U$  calculations were carried out using the projector augmented wave (PAW) method [26,27] and a plane-wave basis as implemented in the Vienna Ab initio Simulation Package (VASP) [28,29]. A kinetic energy cutoff of 500 eV was used and the Brillouin zone of the 40-atom supercell was sampled with a  $6 \times 6 \times 4$   $k$ -point grid in combination with the

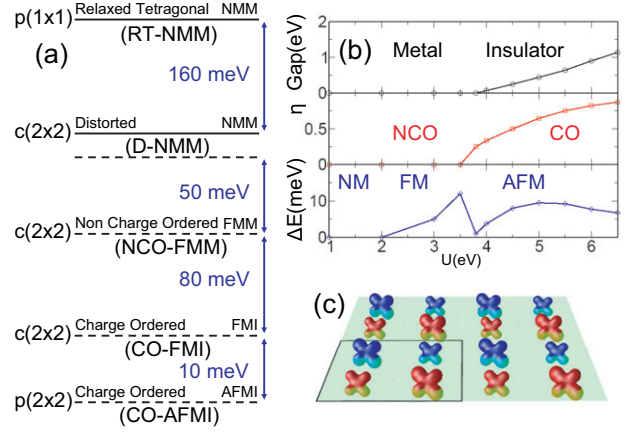


**Fig. 2:** (Colour on-line) (a) Energy gained per surplus electron by relaxing symmetry constraints. The LDA +  $U$  energies (dashed lines) and energy differences calculated here with  $U_d = 5$  eV depend on the value of  $U$  used and so are just indicative. (b) Phase diagram as a function of the value of  $U_d^{\text{Ti}}$ . Top: energy gap. Middle: disproportionation order parameter  $\eta = |n_1 - n_2| / (n_1 + n_2)$ , where  $n_i$  is the occupation of the Ti  $d$  states on ion  $i$ . Bottom:  $\Delta E = |E_{\text{COFM}} - E_{\text{COAFM}}|$ . (c) Spatial magnetic distribution of the COAFM states ( $U_d = 4$  eV) at the interface.

tetrahedron method [30]. Compared to the LDA, the LDA +  $U$  approach gives an improved description of  $d$  electron localization [23]. We use the rotationally invariant LDA +  $U$  method [31] with, unless stated otherwise,  $U_d = 5$  and  $J_d = 0.64$  eV for Ti  $d$  states. The La  $f$  states are forced to lie higher in energy by imposing a large  $U_f = 11$  eV and  $J_f = 0.68$  eV [32].

**Results.** – Because samples are grown on STO substrates, we fix the in-plane lattice constant at the experimental value for STO. This imposes a strain on LAO with a 3% smaller bulk lattice constant. Our starting point is a fully relaxed, tetragonal, non-magnetic metallic (RT-NMM)  $p(1 \times 1)$  configuration. We then remove symmetry constraints to obtain, in order of increasing energy gain (fig. 2a): a  $c(2 \times 2)$  distorted non-magnetic metallic (D-NMM) structure; a metastable spin-polarized, non-charge-ordered (NCO) state, with a single interface-Ti charge state, obtained by switching on  $U_d^{\text{Ti}}$ ; a charge-ordered ferromagnetic insulating (CO-FMI) state with an energy gap of 0.44 eV in which the Ti sites are not equivalent (fig. 1); a  $p(2 \times 2)$  charge-ordered anti-ferromagnetic insulating state (CO-AFMI).

The charge transferred from LAO to the smaller band gap STO is bound close to the interface. As predicted by Okamoto and Millis [18] and confirmed for LTO|STO interfaces using calculations similar to those presented here [32], the effect of lattice relaxation is to smooth the potential discontinuity and allow charge to leak into the bulk-like STO. For our NCO-FMM state, the occupied part of the bottom of the conduction band is almost 1 eV

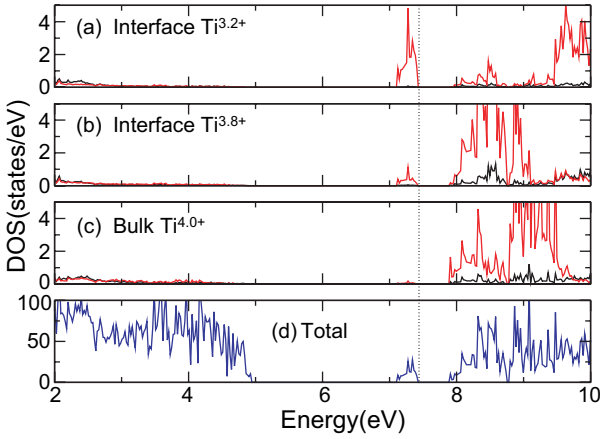


Fig. 3: (Colour on-line) Interface densities of states (DoS) for the lowest-energy charge-ordered antiferromagnetic insulating (CO-AFMI) configuration. (a), (b) Projected 3d DoS of (nominally)  $\text{Ti}^{3+}$  and  $\text{Ti}^{4+}$  interface Ti ions. The transferred electron has  $t_{2g}$  (red) character with the  $e_g$  states (black) far above the Fermi energy. (c) Projected 3d DoS of bulk  $\text{Ti}^{4+}$  ions; (d) total DoS.

wide and we confirm the occurrence of charge leakage at the LAO|STO interface.

The NCO-FMM state is unstable with respect to charge disproportionation [11] into inequivalent  $\text{Ti}^{3.2+}$  and  $\text{Ti}^{3.8+}$  interface ions as a result of the Coulomb repulsion and spin polarization on the Ti ions favouring integer occupancy; the transferred electron is localized on the nominally 3+ interface  $\text{Ti}^{3+}$  ions with little leakage into bulk STO (fig. 3). The atoms relax to accommodate the charge ordering: small displacements of the oxygen atoms surrounding the  $\text{Ti}^{3+}$  ion lead to that  $\text{TiO}_6$  octahedron expanding while the other one contracts. The combination of this distortion with the potential barrier and reduced symmetry at the interface leads to one of the Ti  $t_{2g}$  states splitting off completely from the bottom of the STO conduction band and a gap opening up for quarter filling. The transferred electron remains strongly localized at the interface with essentially no leakage into the bulk layer. Because of the  $\text{GdFeO}_3$ -type interface distortion, the occupied Ti  $t_{2g}$  state has  $0.35|xy\rangle + 0.14|yz\rangle + 0.92|xz\rangle$  orbital character (fig. 1).

In a  $p(2 \times 2)$  geometry, the kinetic energy can be further reduced by flipping the spins of equivalent Ti ions in a checkerboard pattern. The bandwidth is narrowed from 0.7 to 0.4 eV and the energy gap of the CO-AFMI state increased compared to the CO-FMI state. The total energy is lowered but the energy gain  $\sim 10$  meV is small, close to the limit of our accuracy.

The effect of varying  $U_d^{\text{Ti}}$  between 2 and 7 eV, keeping  $J$  fixed at 0.64 eV, is shown in fig. 2b. Between 3.5 and 4 eV, charge disproportionation takes place, AF ordering becomes more favourable and a metal insulator transition occurs. Increasing  $U_d$  leads to a larger CO gap and with increasing charge disproportionation the stripe charge

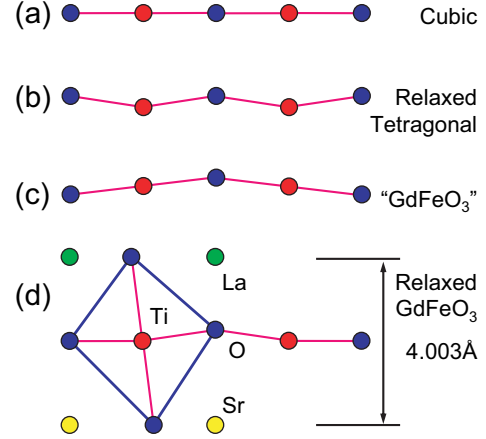


Fig. 4: (Colour on-line) Sketch of the vertical displacement patterns of the Ti and O interface atoms for an ideal cubic structure (a), a relaxed  $p(1 \times 1)$  structure (b), an ideal  $c(2 \times 2)$  “ $\text{GdFeO}_3$ ” structure (c) and the fully relaxed  $c(2 \times 2)$  “buckling” structure (d).

and AF ordered pattern shown in fig. 2c evolves into a checkerboard pattern. The energy difference between CO-FMI and CO-AFMI states reaches a maximum at  $U_d = 5$  eV, the effect of increasing  $U$  being to suppress the exchange coupling between neighbouring spins. The most important result of this study is that the  $\text{TiO}_6$  rotation reduces the bandwidth of the split-off band by about a  $1/3$  (consistent with results found for the bulk  $3d^1$  oxides, ref. [22]) so that very modest values of  $U_d$  result in FM and AFM ordering and a metal insulator (MI) transition close to the FM-AFM phase boundary.

**Structure.** – Because the LAO lattice constant is 3% smaller than that of STO, LAO might be expected to shrink in the  $z$ -direction when it is forced to match in-plane to STO. However, at the interface, we find that the La and Sr planes are separated by 4.003 Å which is substantially larger than  $(3.905 + 3.789)/2$ , the arithmetic average of the LAO and STO lattice constants, and somewhat larger than the lattice constant of a fictitious cubic LTO phase with the same volume as the experimentally observed orthorhombic phase, but consistent with recent experiments [33]. By comparing results for  $(\frac{3}{2}, \frac{5}{2})$  and  $(\frac{5}{2}, \frac{7}{2})$  multilayers for the NCO-FMM and CO-FMI states, we find that the  $\text{GdFeO}_3$  rotation of the  $\text{TiO}_6$  octahedra is confined to the interface. The central STO (LAO) layers in the  $(\frac{5}{2}, \frac{7}{2})$  multilayers are essentially cubic (tetragonal). Compared to a bulk orthorhombic  $\text{LaTiO}_3$  with an appropriately scaled lattice parameter, the shift of the La and Sr ions is reduced, presumably as a result of the constraints imposed by  $\frac{5}{2}$  or  $\frac{7}{2}$  layers of cubic STO and the availability of only half an extra electron in the Ti  $d$  states.

Previous LDA and LDA +  $U$  calculations found ferroelectric-like displacements of negatively charged O and positively charged Ti ions when the geometry was optimized for  $p(1 \times 1)$  structures [12,32] resulting in a



zigzag pattern of O-Ti-O-Ti-O Ti displacements perpendicular to the interface, see fig. 4b. Combining this with the GdFeO<sub>3</sub> rotation of the TiO<sub>6</sub> octahedra (fig. 4c) leads to the buckling pattern shown in fig. 4d in which one oxygen atom is displaced by  $\sim 0.15$  Å out of an otherwise essentially linear chain.

**Discussion.** – To understand the magnetoresistance results reported in ref. [4], we must assume that we are just on the insulating side of the MI transition in fig. 2b i.e.,  $U_d^{\text{Ti}} \sim 4$  eV. Our calculations predict that the strong correlation of Ti *d* states will lead to electrons transferred from the LaO to the TiO<sub>2</sub> layer being trapped on the interface Ti ions in an AFMI state. The localization of these intrinsic carriers would explain the high sheet resistance ( $> 10^4 \Omega/\square$ ) and low carrier concentration ( $\sim 10^{13} \text{ cm}^{-2}$ ) of samples prepared at high oxygen pressure [1,4,6,7]. The existence of a band gap would explain the decrease of sheet resistance with increasing temperature [4]. The application of an external magnetic field would force the AFMI system into a ferromagnetic insulating state with a smaller band gap, leading to a reduced resistance as observed.

This cannot be the whole picture, however. For example, a simple (doped) semiconductor model would predict carrier freeze-out at low temperatures and this is not observed. The role of oxygen vacancies as well as that of the cation mixing at the interface needs to be clarified. If we focus on the ideal of an intrinsic, abrupt interface, perhaps the most pressing issue to be resolved experimentally relates to the appropriate value of  $U_d^{\text{Ti}}$  which is a free parameter in our otherwise parameter-free study. A spectroscopic study identifying the existence and size of the predicted CO gap would be invaluable for making further progress.

**Summary and conclusions.** – Using LDA and LDA+*U* calculations, we have shown that the half-electron (per interface Ti ion) transferred from the LaO layer on one side of an LAO|STO interface to the TiO<sub>2</sub> layer on the other side favours a rotation of TiO<sub>6</sub> octahedra just as it does in bulk LTO. As in bulk LTO, the distortion is crucial to the formation of a charge-ordered AFMI ground state and other charge, magnetic and orbital properties, and results in a characteristic buckling of the Ti-O-Ti bonding at the interface. Ionic relaxation plays a crucial role in determining the localization of the extra electron on the interface Ti ions and leakage into the bulk layer. However, charge ordering suppresses this leakage even when relaxation is included and, in the CO states the electrons are strongly localized at the interface. Our calculations suggest an explanation for recent experimental results in terms of the proximity of an AFMI ground state to a FMM excited state (or a FMI state with reduced band gap). With only half an electron trapped in an otherwise empty Ti *d* orbital, the LAO|STO interface is an attractive object for quarter-filled Hubbard model studies.

\*\*\*

This work is supported by “NanoNed”, a nanotechnology programme of the Dutch Ministry of Economic Affairs. Use of supercomputer facilities was sponsored by the “Stichting Nationale Computer Faciliteiten” (NCF) financially supported by the “Nederlandse Organisatie voor Wetenschappelijk Onderzoek” (NWO). The authors thank P. X. XU, Q. F. ZHANG, D. VANPOUCKE, S. KUMAR, A. BRINKMAN and G. RIJNDERS for useful discussions.

## REFERENCES

- [1] OHTOMO A. and HWANG H. Y., *Nature*, **427** (2004) 423.
- [2] HUIJBEN M., RIJNDERS G., BLANK D. H. A., BALS S., AERT S. V., VERBEECK J., TENDELOO G. V., BRINKMAN A. and HILGENKAMP H., *Nat. Mater.*, **5** (2006) 556.
- [3] THIEL S., HAMMERL G., SCHMEHL A., SCHNEIDER C. W. and MANNHART J., *Science*, **313** (2006) 1942.
- [4] BRINKMAN A., HUIJBEN M., VAN ZALK M., HUIJBEN J., ZEITLER U., MAAN J. C., VAN DER WIEL W. G., RIJNDERS G., BLANK D. H. A. and HILGENKAMP H., *Nat. Mater.*, **6** (2007) 493.
- [5] REYREN N., THIEL S., CAVIGLIA A. D., KOURKOUTIS L. F., HAMMER G., RICHTER C., SCHNEIDER C. W., KOPP T. and RÜETSCHI A.-S., JACCARD D. *et al.*, *Science*, **317** (2007) 1196.
- [6] HERRANZ G., BASLETIC M., BIBES M., CARRÉTÉRO C., TAFRA E., JACQUET E., BOUZEHOUE K., DERANLOT C. and HAMZIC A., BROTO J.-M. *et al.*, *Phys. Rev. Lett.*, **98** (2007) 216803.
- [7] SIEMONS W., KOSTER G., YAMAMOTO H., HARRISON W. A., LUCOVSKY G., GEBALLE T. H., BLANK D. H. A. and BEASLEY M. R., *Phys. Rev. Lett.*, **98** (2007) 196802.
- [8] WILLMOTT P. R., PAULI S. A., HERGER R., SCHLEPÜTZ C. M., MARTOCCIA D., PATTERSON B. D., DELLEY B., CLARKE R., KUMAR D. and CIONCA C. *et al.*, *Phys. Rev. Lett.*, **99** (2007) 155502.
- [9] KALABUKHOV A., GUNNARSSON R., BÖRJESSON J., OLSSON E., CLAESON T. and WINKLER D., *Phys. Rev. B*, **75** (2007) 121404(R).
- [10] BASLETIC M., MAURICE J.-L., CARRÉTÉRO C., HERRANZ G., COPIE O., BIBES M., JACQUET E., BOUZEHOUE K., FUSIL S. and BARTHÉLÉMY A., *Nat. Mater.*, **7** (2008) 621.
- [11] PENTCHEVA R. and PICKETT W. E., *Phys. Rev. B*, **74** (2006) 035112.
- [12] PARK M. S., RHIM S. H. and FREEMAN A. J., *Phys. Rev. B*, **74** (2006) 205416.
- [13] CEN C., THIEL S., HAMMERL G., SCHNEIDER C. W., ANDERSEN K. E., HELMBERG C. S., MANNHART J. and LEVY J., *Nat. Mater.*, **7** (2008) 298.
- [14] MACLEAN D. A., NG H.-N. and GREEDAN J. E., *J. Solid State Chem.*, **30** (1979) 35.
- [15] CWIK M., LORENZ T., BAIER J., MÜLLER R., ANDRÉ G., BOURÉE F., LICHTENBERG F., FREIMUTH A. and SCHMITZ R., MÜLLER-HARTMANN E. *et al.*, *Phys. Rev. B*, **68** (2003) 060401(R).
- [16] HEMBERGER J., VON NIDDA H.-A. K., FRITSCH V., DEISENHOFER J., LOBINA S., RUDOLF T., LUNKENHEIMER P., LICHTENBERG F. and LOIDL A., BRUNS D. *et al.*, *Phys. Rev. Lett.*, **91** (2003) 066403.

- [17] OKIMOTO Y., KATSUFUJI T., OKADA Y., ARIMA T. and TOKURA Y., *Phys. Rev. B*, **51** (1995) 9581.
- [18] OKAMOTO S. and MILLIS A. J., *Nature*, **428** (2004) 630.
- [19] LEE W.-C. and MACDONALD A. H., *Phys. Rev. B*, **76** (2007) 075339.
- [20] ALBINA J.-M., MROVEC M., MEYER B. and ELSÄSSER C., *Phys. Rev. B*, **76** (2007) 165103.
- [21] RABE K. M. and GHOSEZ P., *Top. Appl. Phys.*, **105** (2007) 117.
- [22] PAVARINI E., YAMASAKI A., NUSS J. and ANDERSEN O. K., *New J. Phys.*, **7** (2005) 188.
- [23] ANISIMOV V. I., ARYASETIWAN F. and LICHTENSTEIN A. I., *J. Phys.: Condens. Matter*, **9** (1997) 767.
- [24] OKATOV S., POTERYAEV A. and LICHTENSTEIN A., *Europhys. Lett.*, **70** (2005) 499.
- [25] ZHONG Z. and KELLY P. J., to be submitted to *Phys. Rev. B* (2008).
- [26] BLÖCHL P. E., *Phys. Rev. B*, **50** (1994) 17953.
- [27] KRESSE G. and JOUBERT D., *Phys. Rev. B*, **59** (1999) 1758.
- [28] KRESSE G. and HAFNER J., *Phys. Rev. B*, **47** (1993) 558.
- [29] KRESSE G. and FURTHMULLER J., *Phys. Rev. B*, **54** (1996) 11169.
- [30] BLÖCHL P. E., JEPSEN O. and ANDERSEN O. K., *Phys. Rev. B*, **49** (1994) 16223.
- [31] DUDAREV S. L., BOTTON G. A., SAVRASOV S. Y., HUMPHREYS C. J. and SUTTON A. P., *Phys. Rev. B*, **57** (1998) 1505.
- [32] OKAMOTO S., MILLIS A. J. and SPALDIN N. A., *Phys. Rev. Lett.*, **97** (2006) 056802.
- [33] VONK V., HUIJBEN M., DRIESSEN K. J. I., TINNEMANS P., BRINKMAN A., HARKEMA S. and GRAAFSMA H., *Phys. Rev. B*, **75** (2007) 235417.